CEE598/CEE526/MAE527
Finite Element for Engineers

FE Modeling Case Studies

S. D. Rajan
Department of Civil Engineering
Arizona State University
Tempe, AZ 85287

Latest Revision: October 2008

Table of Contents

Section		*Page*
1	Thin Cantilever Beam	3
2	72” Pipe Crossing	9
3	References	19

1 Finite Element Analysis of a Thin Cantilever Beam

1.1 Problem Description

The structure in question is a $6" \times 0.8" \times 0.1"$ thin cantilever steel plate subjected to a tip (in-plane) loading as shown in Fig. 1.1. The problem is a slight modification of the problem from Ref. [2]. The objectives of the analysis are to track (a) the largest vertical displacement that occurs along CD and (b) σ_x at point A. The finite element analysis is carried out using HYI-3D [1] program.

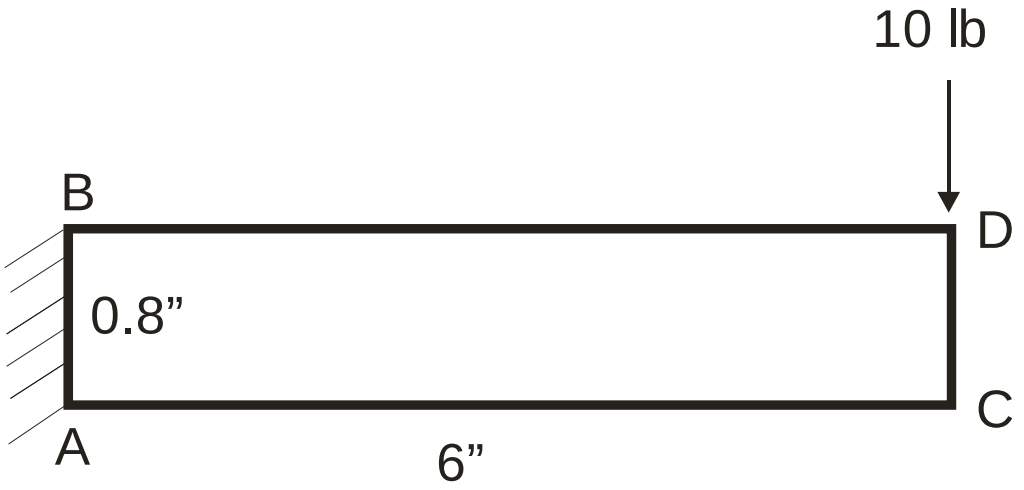

Fig. 1.1 Cantilever beam with tip loading

1.2 Finite Element Model

Type of analysis: The FE model is a two-dimensional model representing plane stress conditions. A small displacement, small strain, materially linear and isotropic, static loading finite element analysis is carried out. The finite element domain is shown in Fig. 1.2.

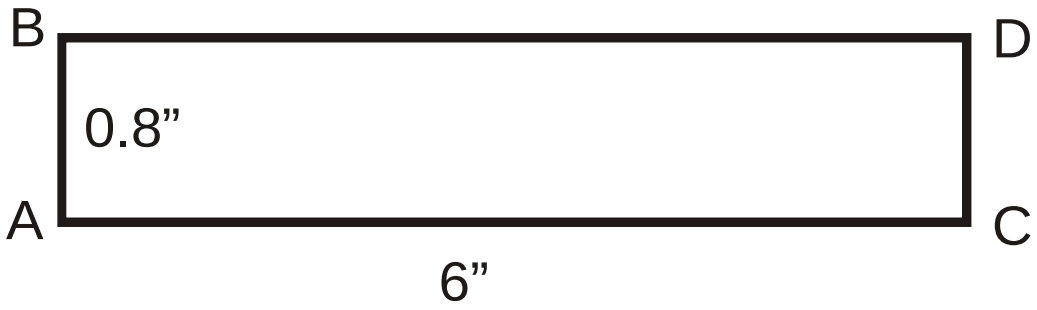

Fig. 1.2 Schematic diagram of the finite element domain

Material properties: The material values used in the analysis are as follows.

(a) The modulus of elasticity of the plate is 30×10^6 *psi* .

(b) The Poisson’s ratio is 0.3.

Loading: We will start by applying a point load at D.
Fixity Conditions: We will assume that all the finite element nodes on edge AB are restrained (fixed) in the x and y directions (Fig. 1.3).

Fig. 1.3 Fixity conditions

Choice of finite element: We will study the performance of first-order and second-order finite elements.

Simple Beam Theory Approximate Solution: Simple beam theory results are as follows.

$$\Delta = \frac{PL^3}{3EI} = \frac{(10)(6)^3}{3\left(30\times10^6\right)\left(\frac{0.1\times0.8^3}{12}\right)} = 0.005625\,\text{in}$$

$$\sigma = \frac{Mc}{I} = \frac{(10)(6)(0.4)}{\left(\frac{0.1\times0.8^3}{12}\right)} = 5625\ psi$$

It will be helpful to recall the assumptions made in the SBT analysis.

1.3 Results
When the 10 lb load is applied as a point load, we obtain the stress distribution as shown in Fig. 1.4.

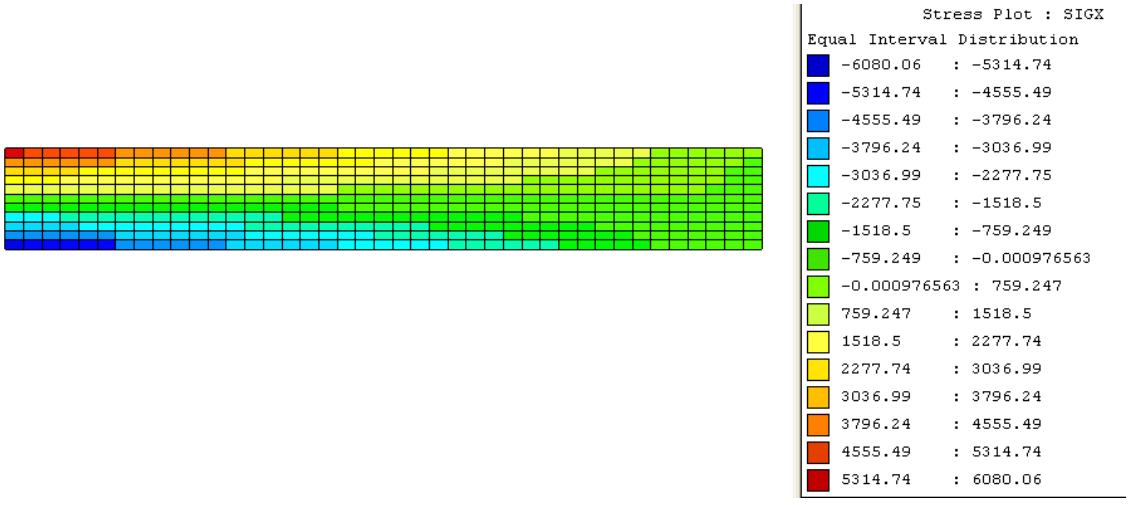

Fig. 1.4 σ_x stress distribution

Note the high stress values in the vicinity of the loads. In order to mimic the SBT assumptions, we will now apply the load as a surface traction of $12.5 lb/in$ on edge CD. The results from successive mesh refinements are shown in Table 1.1. The meshes are labeled 1 through 5 are shown in Fig. 1.5(a)-(e).

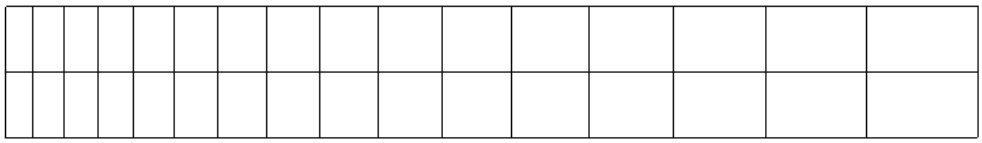

Fig. 1.5(a) Mesh –1

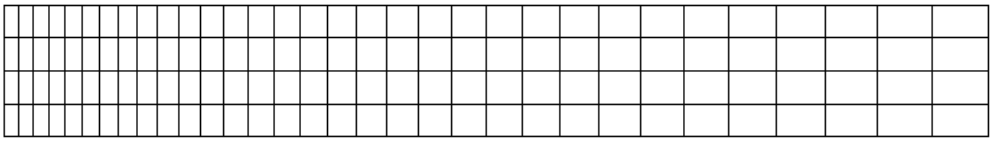

Fig. 1.5(b) Mesh –2

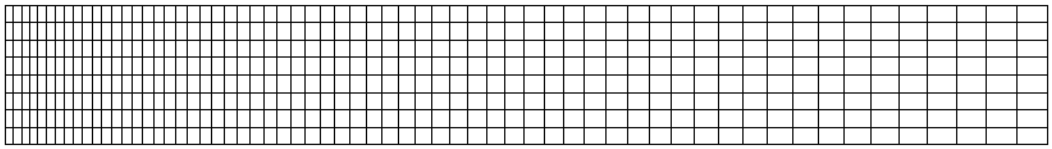

Fig. 1.5(c) Mesh –3

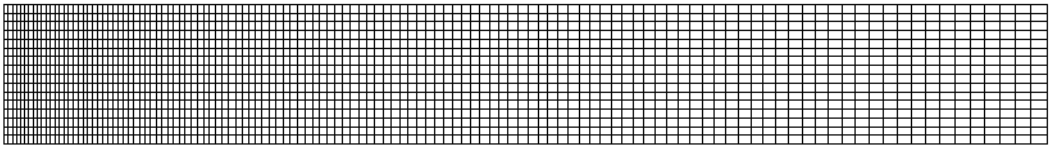

Fig. 1.5(d) Mesh –4

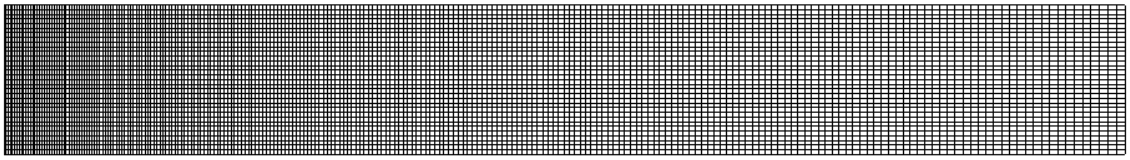

Fig. 1.5(e) Mesh –5

Table 1.1 Results from the FE Analyses

Model	Element Type	Number of nodes	Number of elements	Tip displacement (in)	$(\sigma_x)_A$ (psi)
Q4CantBeam-1	Q4	51	32	-0.0046	4535
Q4CantBeam-2	Q4	165	128	-0.0050	5524
Q4CantBeam-3	Q4	567	496	-0.0051	6358
Q4CantBeam-4	Q4	2091	1952	-0.00516	7352
Q4CantBeam-5	Q4	8019	7744	-0.00517	8668

While the tip displacement shows a converging trend, the stress $(\sigma_x)_A$ appears to be increasing with increasing mesh refinement. This is because the nodes on edge AB are constrained in both the x and y directions. Hence point A that should show a stress distribution trend of the form $\sigma_y = \tau_{xy} \to 0$ with increasing mesh refinement, is no longer true. We need to relax this fixity condition and remove the fixity in the vertical direction. To suppress the rigid body mode, we will restrain one node (at the center of the beam along AB) in both the x and y directions.

In the following analyses, we will use the modified fixity conditions as shown in Fig. 1.6.

Fig. 1.6 Modified fixity conditions

Table 1.2 shows the results when Q4 elements are used.

Table 1.2 Results from the FE Analyses

Model	Element Type	Number of nodes	Number of elements	Tip displacement (in)	$(\sigma_x)_A$ (psi)
Q4CantBeam-1A	Q4	51	32	-0.00467	4475
Q4CantBeam-2A	Q4	165	128	-0.00506	5112
Q4CantBeam-3A	Q4	567	496	-0.00517	5435
Q4CantBeam-4A	Q4	2091	1952	-0.00519	5577
Q4CantBeam-5A	Q4	8019	7744	-0.0052	5643

Fig. 1.7 shows the $(\sigma_x)_A$ stress distribution for Q4CantBeam-5A model.

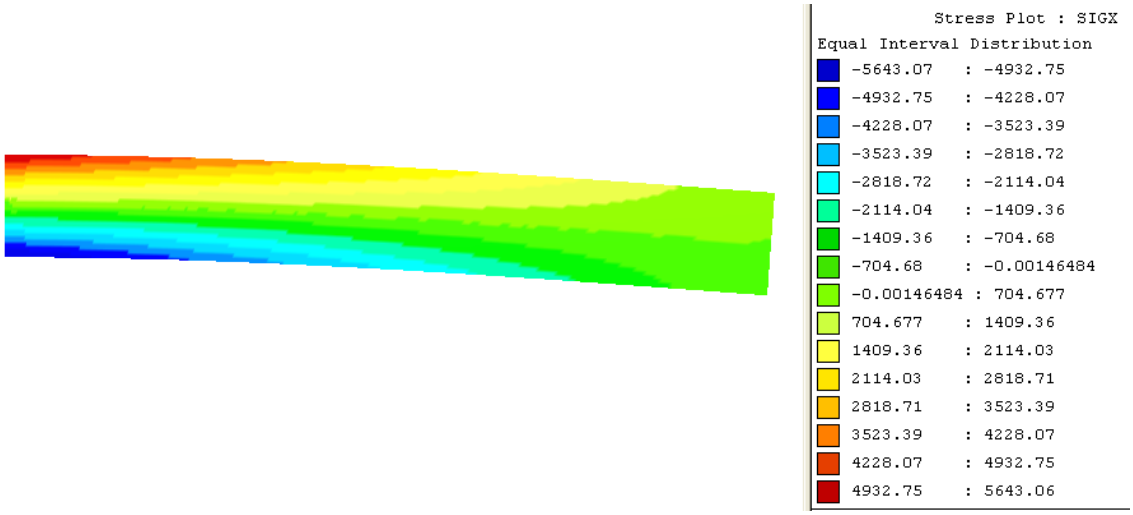

Fig. 1.7 $(\sigma_x)_A$ distribution for Q4CantBeam-5A model

Table 1.3 shows the results when T3 elements are used.

Table 1.3 Results from the FE Analyses

Model	**Element Type**	**Number of nodes**	**Number of elements**	**Tip displacement (in)**	$(\sigma_x)_A$ **(psi)**
T3CantBeam-1A	T3	51	64	-0.00338	3741
T3CantBeam-2A	T3	165	256	-0.0046	5068
T3CantBeam-3A	T3	567	992	-0.0050	5543
T3CantBeam-4A	T3	2091	3904	-0.0052	5673
T3CantBeam-5A	T3	8019	15488	-0.0052	5702

Fig. 1.8 shows the $(\sigma_x)_A$ stress distribution for T3CantBeam-5A model.

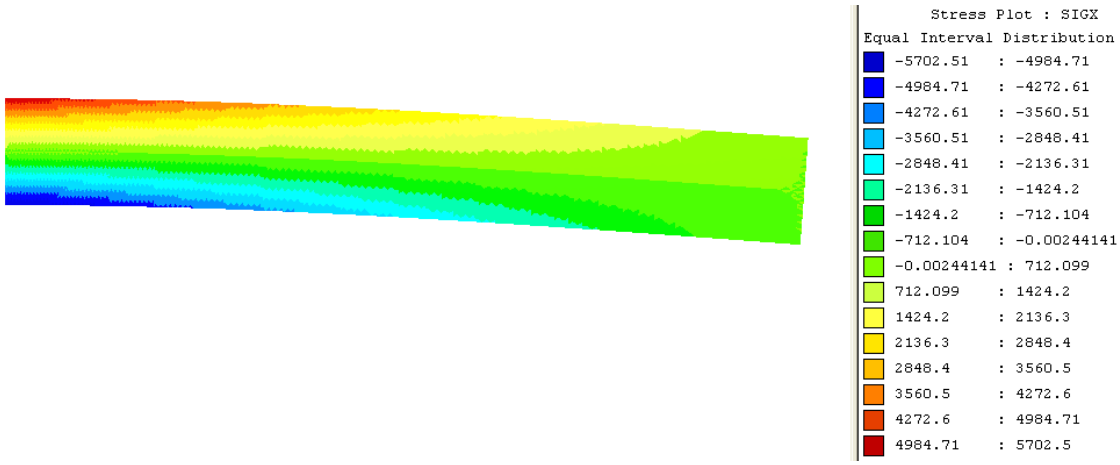

Fig. 1.8 $(\sigma_x)_A$ distribution for T3CantBeam-5A model

Finally, Table 1.4 shows the results when Q8 elements are used.

Table 1.4 Results from the FE Analyses

Model	Element Type	Number of nodes	Number of elements	Tip displacement (in)	$(\sigma_x)_A$ (psi)
Q9CantBeam-1A	Q8	51	8	-0.0052	4352
Q9CantBeam-2A	Q8	165	32	-0.0052	5075
Q9CantBeam-3A	Q8	567	124	-0.0052	5371
Q9CantBeam-4A	Q8	2091	488	-0.0052	5526
Q9CantBeam-5A	Q8	8019	1936	-0.0052	5615

Fig. 1.9 shows the $(\sigma_x)_A$ stress distribution for Q9CantBeam-5A model.

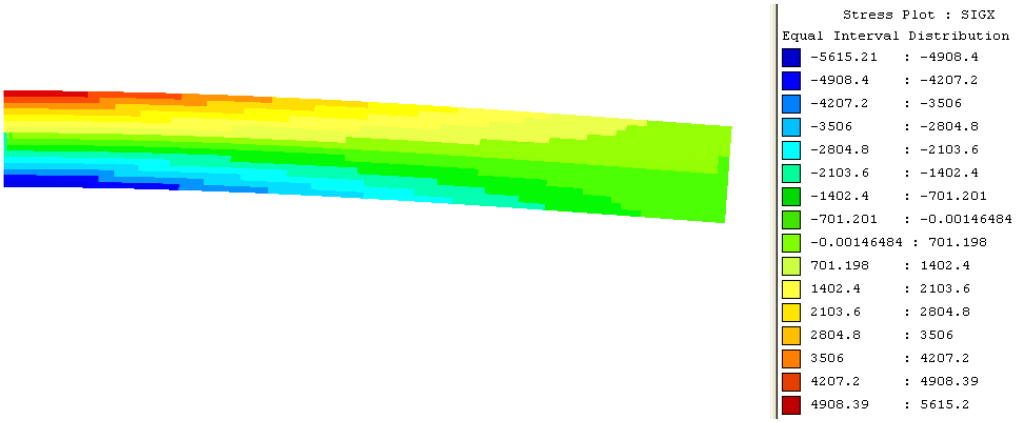

Fig. 1.9 $(\sigma_x)_A$ distribution for Q9CantBeam-5A model

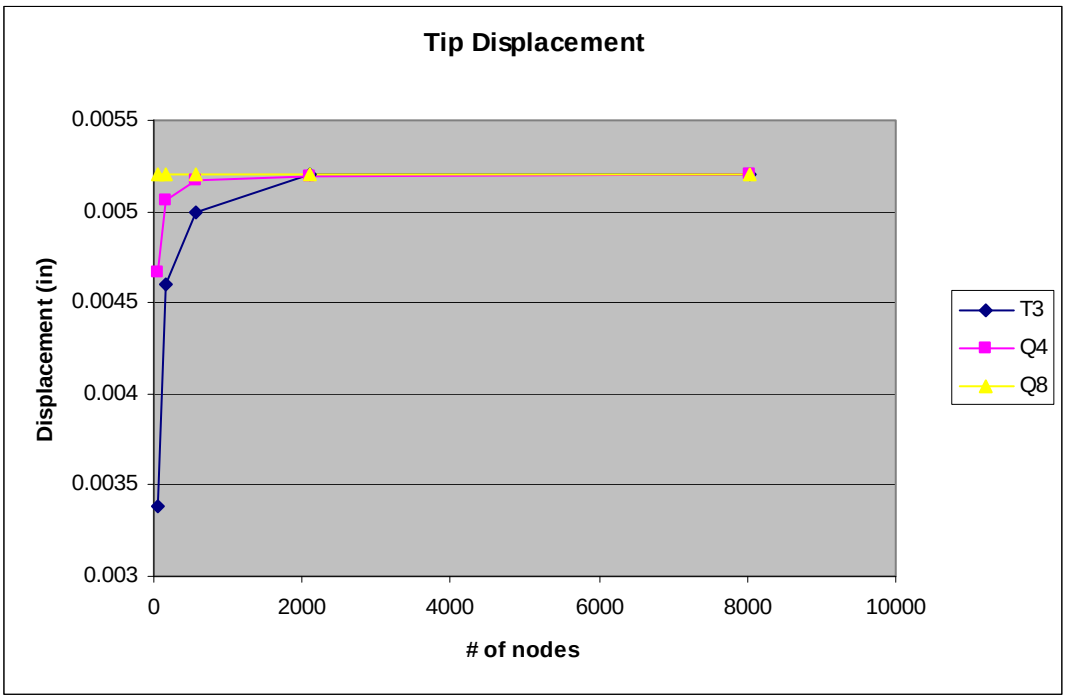

Fig. 1.10 Tip Displacement versus # of Nodes

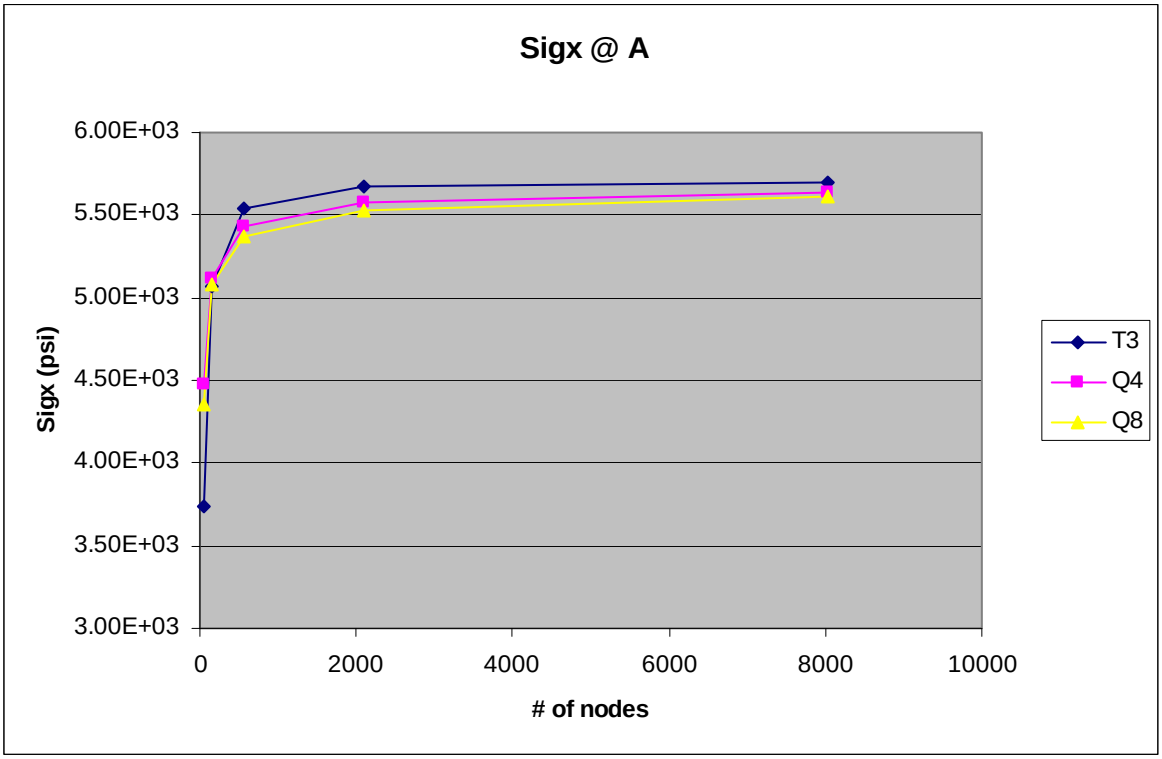

Fig. 1.11 $\left(\sigma_x\right)_A$ versus # of Nodes

1.4 Conclusions

The following observations can be made from the above finite element analyses.

(a) Displacements converge faster than stresses.

(b) Both displacements and stresses converge from below. In other words, the displacements and stresses are underestimated.

(c) Higher-order elements converge faster than lower-order elements.

2 Finite Element Analysis of 72” Pipe Crossing

2.1 Problem Description

The structure in question is a 2-barrel 72” I.D. (86” O.D.) pipe. The objective of the finite element (FE) analysis is to determine the response of cast-in-place plain (unreinforced) concrete pipe subjected to service loads (Fig. 1). The finite element analysis is carried out using HYI-3D [1] program.

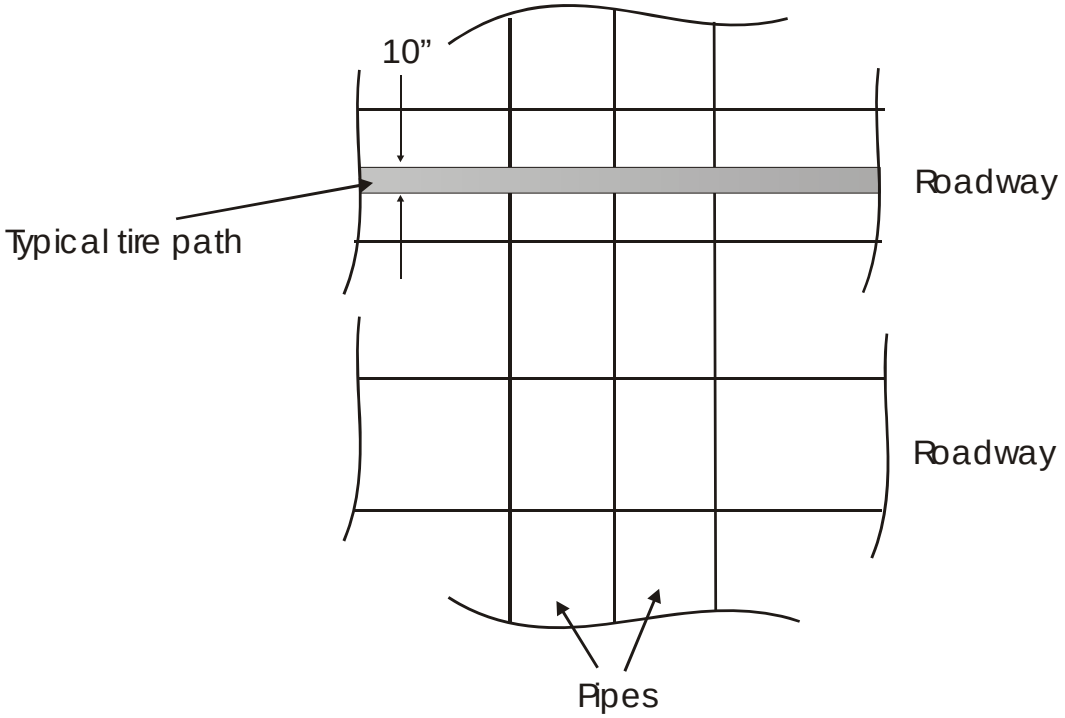

Fig. 1 Plan view showing the pipes and roadway over the pipes

2.2 Finite Element Model

Type of analysis: The FE model is a two-dimensional model representing plane strain conditions. A small displacement, small strain, materially linear and isotropic, static loading finite element analysis is carried out. The finite element domain is shown in Fig. 2.

Material properties: The material values used in the analysis are as follows [3, 4].

(a) Unit weight of soil is taken as 125 pcf.
(b) Unit weight of concrete is taken as 150 pcf.
(c) The modulus of elasticity of native soil is taken to be between 2 500 (representing average of 2 000 and 3 000 psi).
(d) The modulus of elasticity of backfill is taken to be 1 500 psi. Backfill is assumed to cover a distance of $2 \times 87" = 174"$ directly over the two pipes.
(e) The modulus of elasticity of concrete is taken to be 3.8 million psi.
(f) The Poisson’s Ratio of soil is taken as 0.25 and for concrete is taken as 0.15.

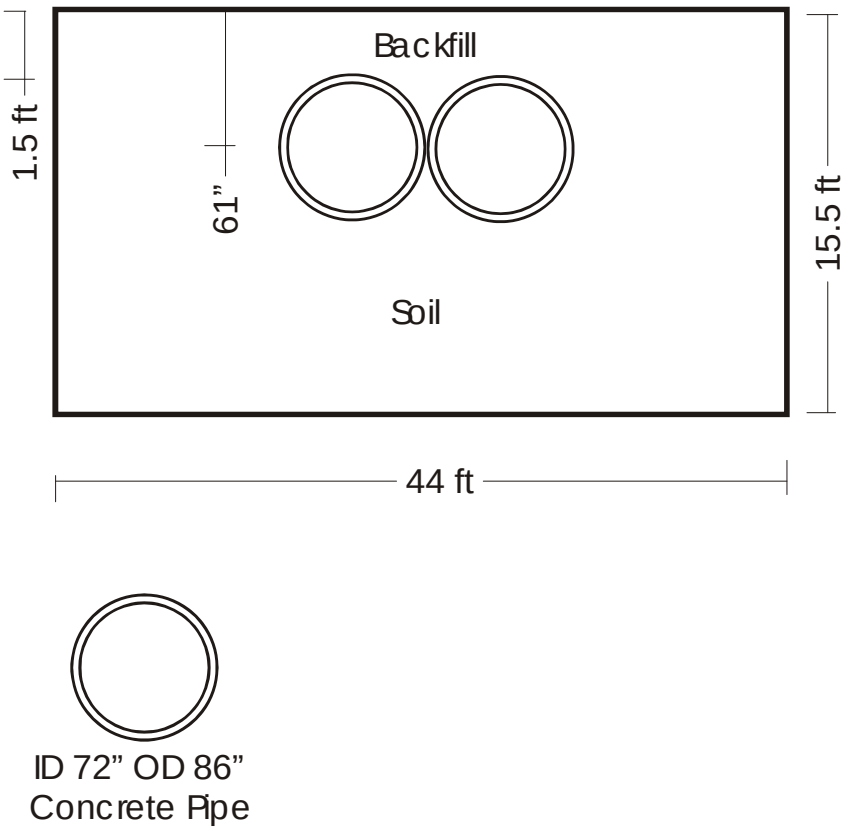

Fig. 2 Schematic diagram of the structural system represented as a two-dimensional model

Loading: The loading on the pipes is due to vehicular and gravitational loading. The HS20-44 wheel loads are taken. The tire profile in contact with the soil is taken to be 10” x 20”. The axle load is taken as 16 000 lbs. A 20% impact is included in the analysis. Two loading conditions are considered. The first loading condition is taken as the equivalent axle load acting directly over the crown of one of the pipes. The second loading condition is taken as the equivalent axle load acting directly over the midpoint between the two pipes.

Since the height of the fill is 1.5 ft, the load distribution length is 2.635 ft. The equivalent planar loading, q (for a unit depth) is computed as follows.

$$q = \frac{16000\,lb}{2.635\,ft \times \frac{12\,in}{1\,ft}} = 506\,\frac{lb}{in} \tag{1}$$

The loading, w is assumed to act on the tire span of 20” and can be computed as

$$w = 1.2\,\frac{q}{20\,in} = \frac{607\,lb/in}{20\,in} = 30.4\,psi \tag{2}$$

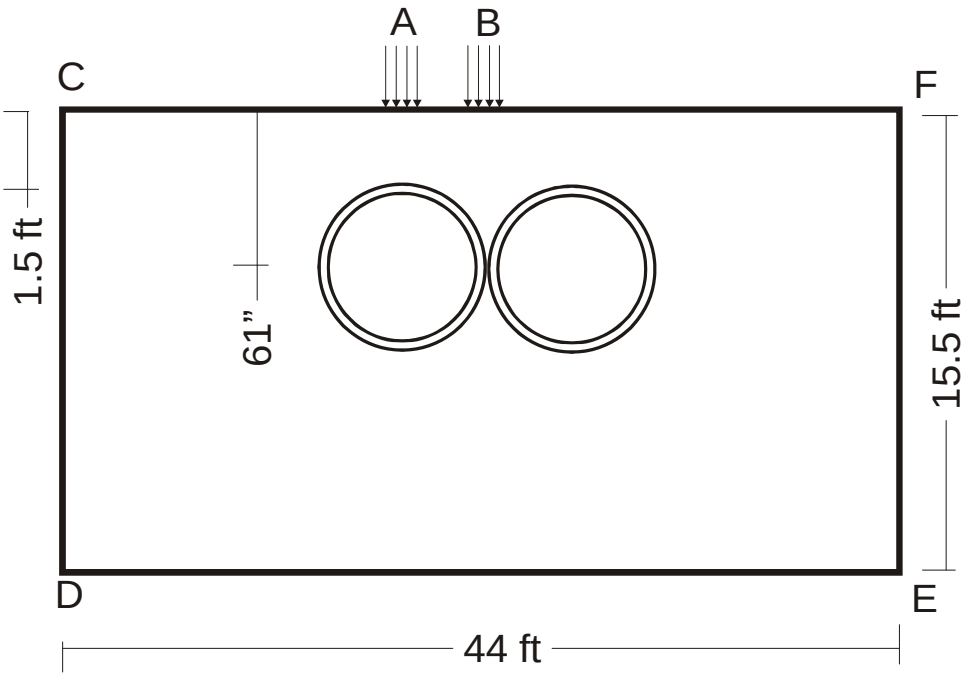

Fig. 3 Load cases considered (a) A represents the first load case (b) B represents the second load case. Distributed loading is applied over a span of 20”

Fixity Conditions: The X and Y displacements are constrained (or fixed) on sides, CD, DE and EF. The displacements are assumed to be negligible beyond these lines. Perfect bonding is assumed between the soil and the pipes. It is also assumed that two pipes are always in contact (act as an integral unit).

Choice of finite element: A plane strain model is assumed and 3-noded triangular (CST) elements are used in the FE model. Higher-order elements (6-noded triangular elements) could have been used. However, the sharp region between the two pipes makes the task of mesh generation difficult.

2.3 Results

Two models were analyzed. The first model is a relatively coarse model (Fig. 4) while the second model is finer in the region represented by the pipes and the backfill (Fig. 5). Details of the two models as well as the results from the FE analyses are shown in Tables 1 and 2.

Table 1 Results from the FE Analyses (Load Case 1)

Model	Number of nodes	Number of elements	Max. Tensile Stress in the Pipe (psi)	Max. Compressive Stress in the Pipe (psi)
Coarse	4630	8467	208	218
Fine	15191	27397	437	425

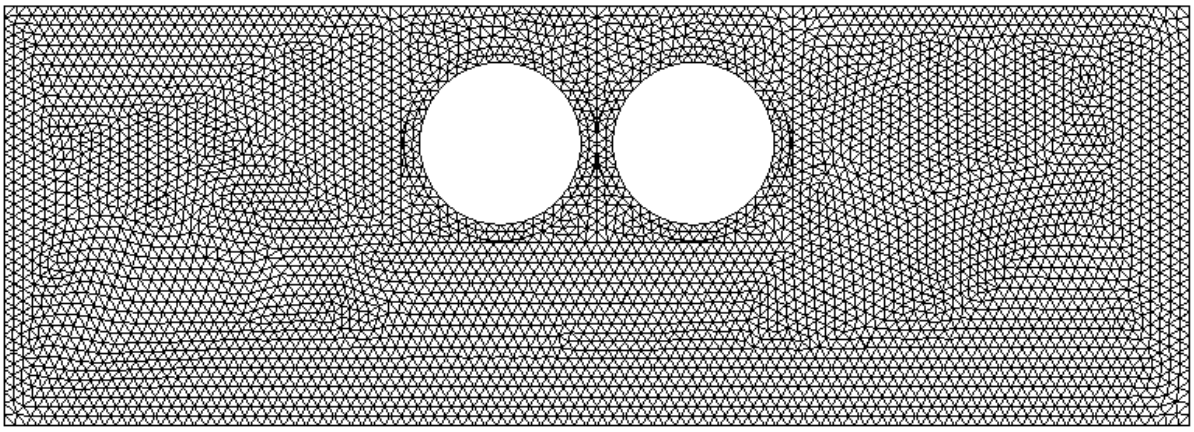

Fig. 4 Coarse FE Model

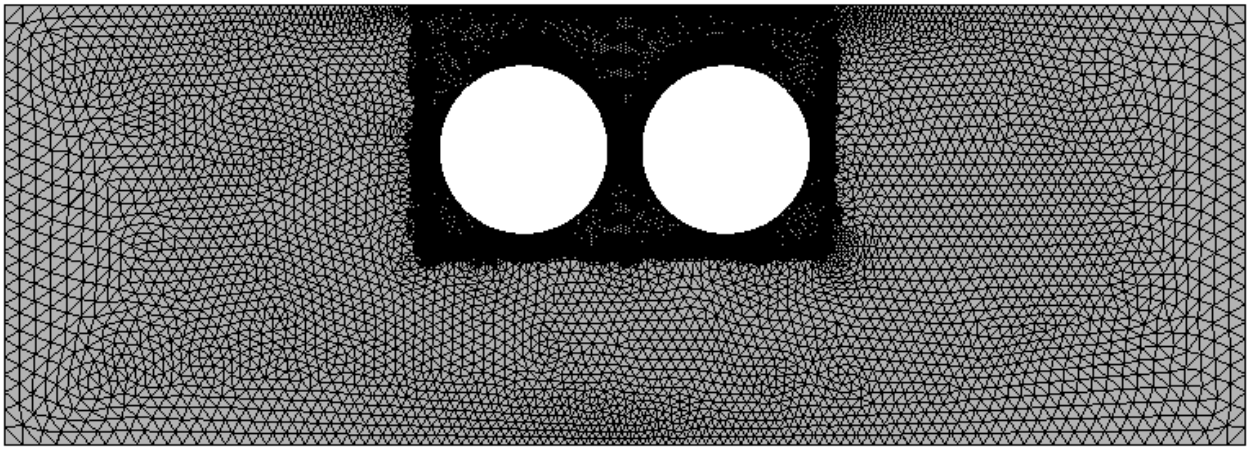

Fig. 5 Fine FE Model

Table 2 Results from the FE Analyses (Load Case 2)

Model	Number of nodes	Number of elements	Max. Tensile Stress in the Pipe (psi)	Max. Compressive Stress in the Pipe (psi)
Coarse	4630	8467	156	217
Fine	15191	27397	356	369

Principal stress plots for the Coarse Model are shown in Fig. 5(a) and 5(b) (Load Case 1) and Fig. 5(c) and 5(d) (Load Case 2). Principal stress plots for the Fine Model are shown in Fig. 6(a) and 6(b) (Load Case 1) and Fig. 6(c) and 6(d) (Load Case 2).

Note the stress legend/scales (that appear in the right pane) for each of the plots.

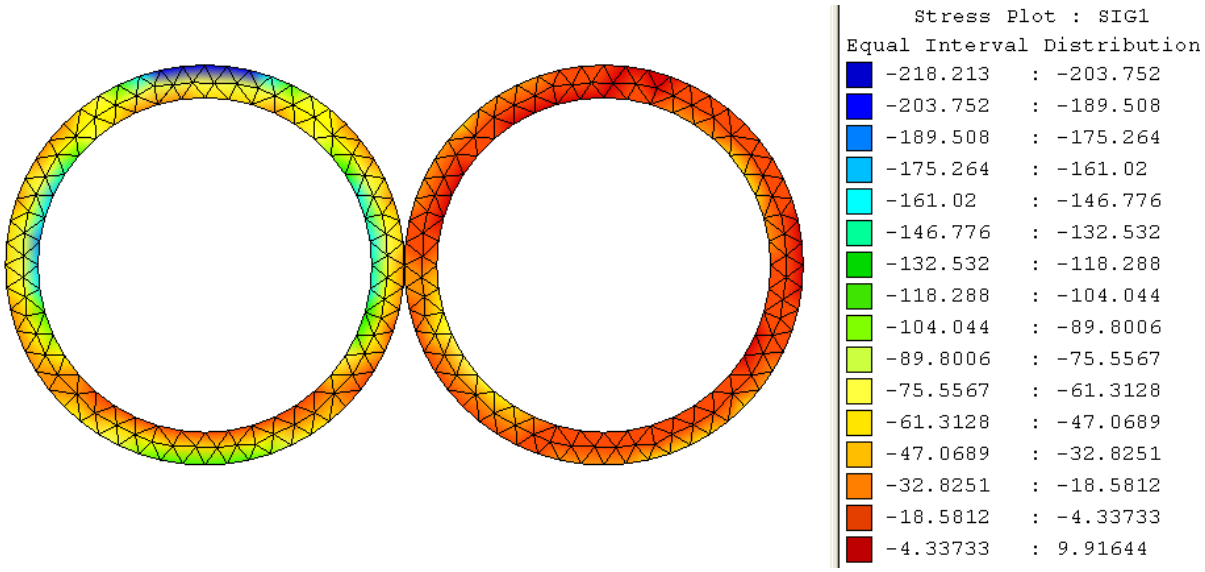

Fig. 5(a) Principal Stress Plot (Largest Compressive Stress) for Load Case 1

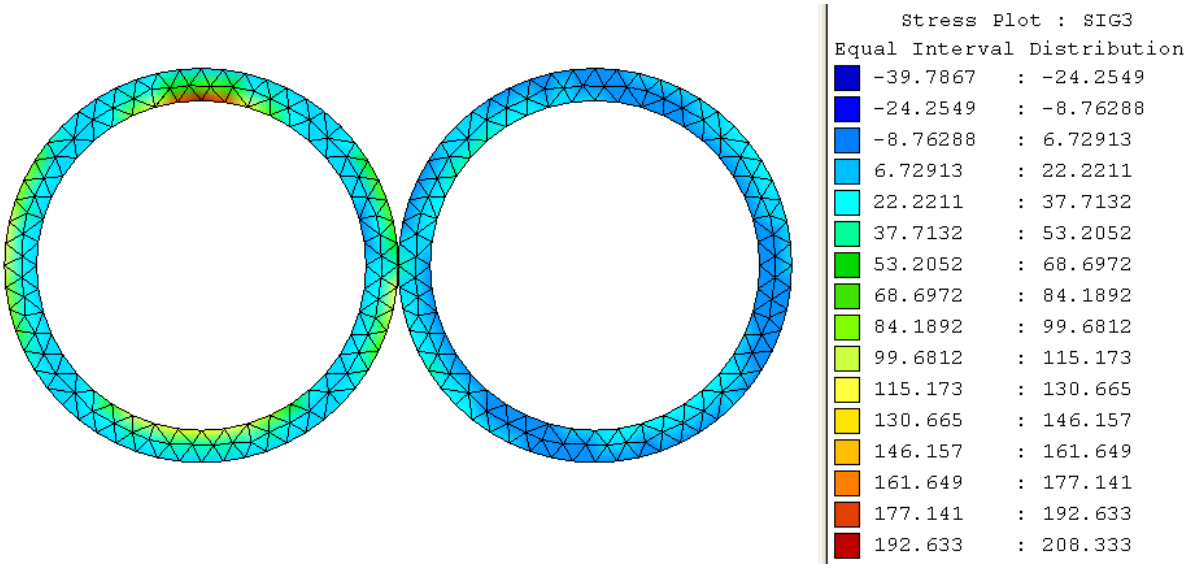

Fig. 5(b) Principal Stress Plot (Largest Tensile Stress) for Load Case 1

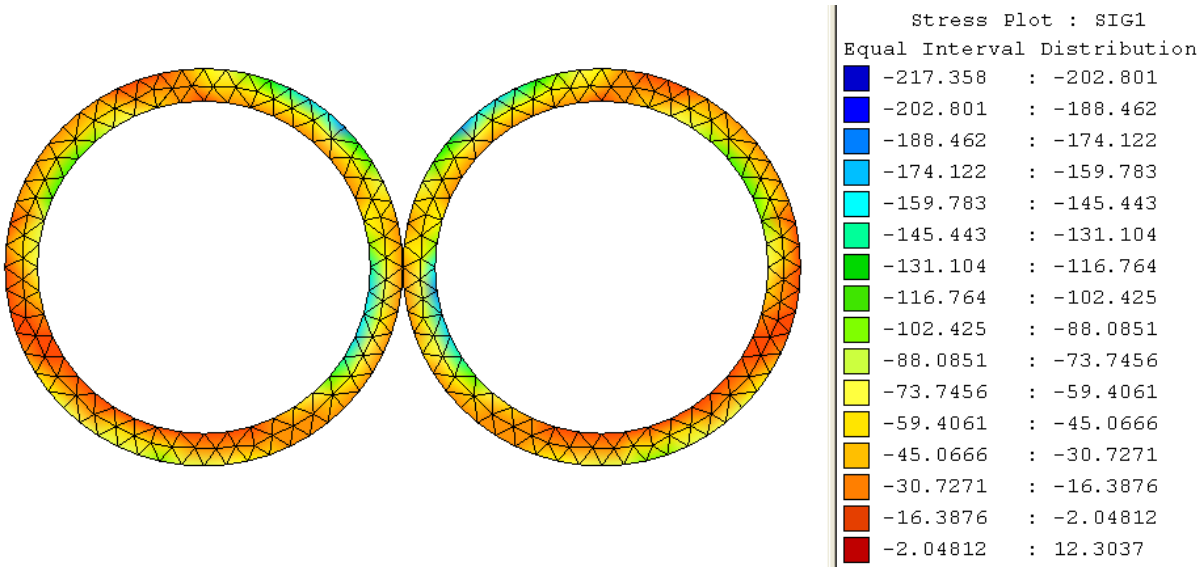

Fig. 5(c) Principal Stress Plot (Largest Compressive Stress) for Load Case 2

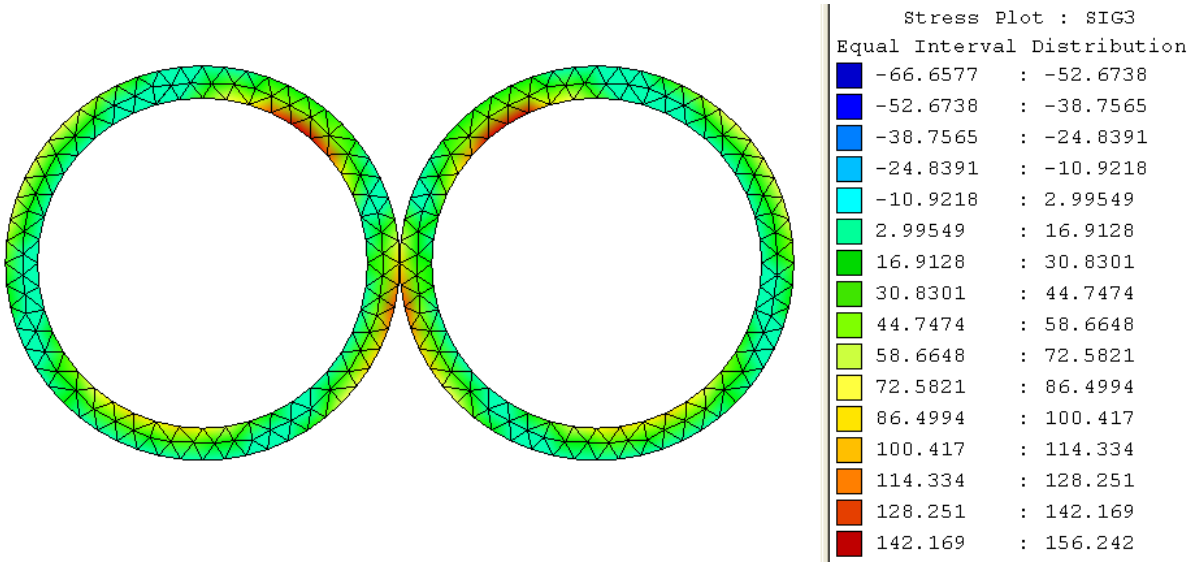

Fig. 5(d) Principal Stress Plot (Largest Tensile Stress) for Load Case 2

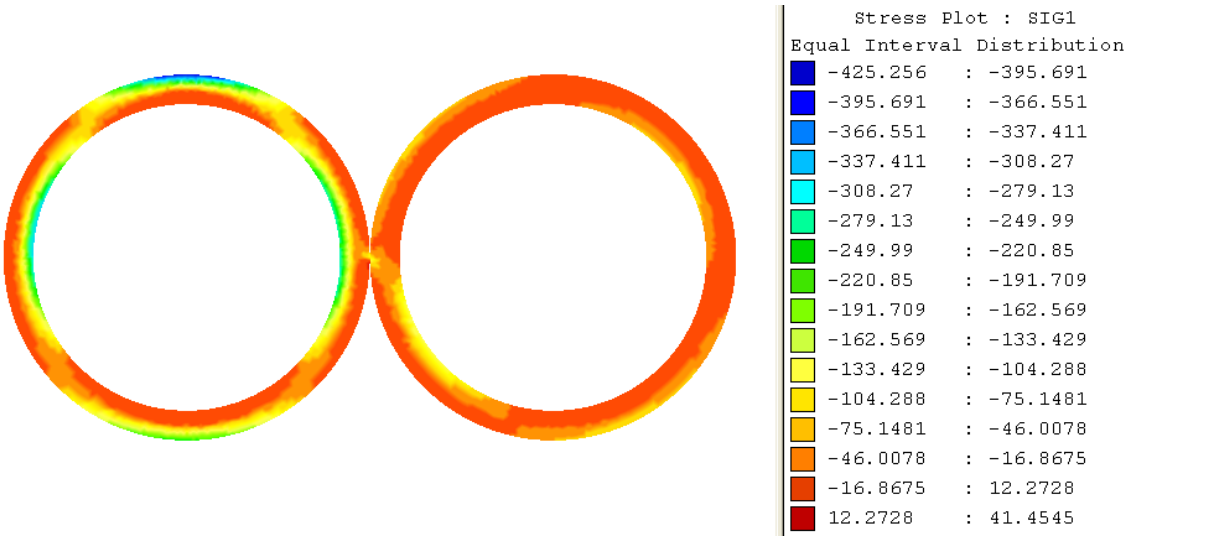

Fig. 6(a) Principal Stress Plot (Largest Compressive Stress) for Load Case 1

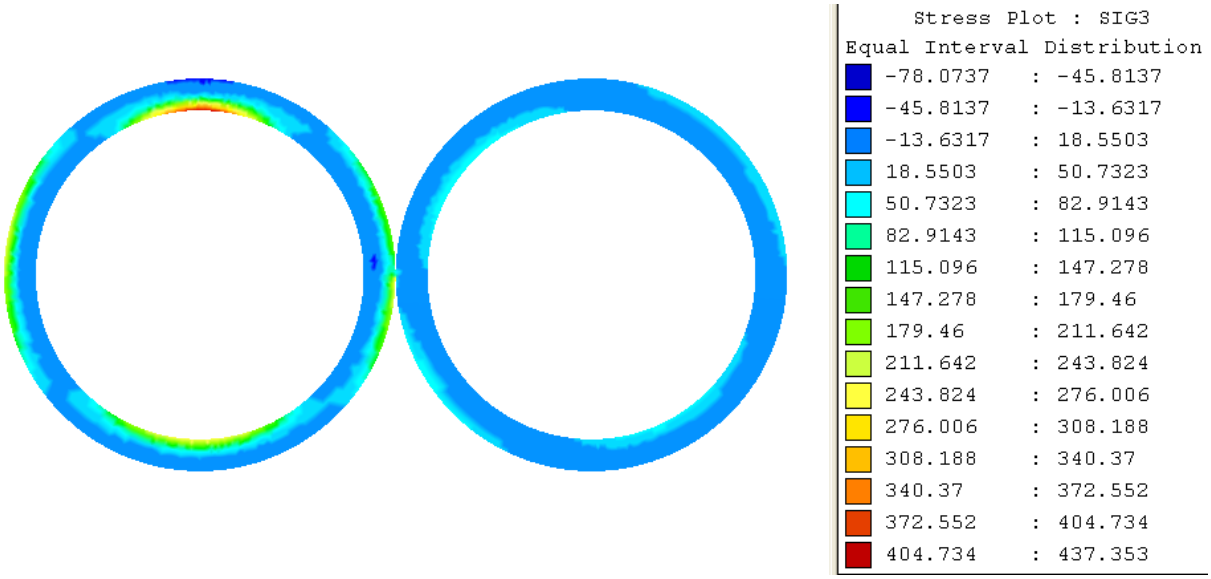

Fig. 6(b) Principal Stress Plot (Largest Tensile Stress) for Load Case 1

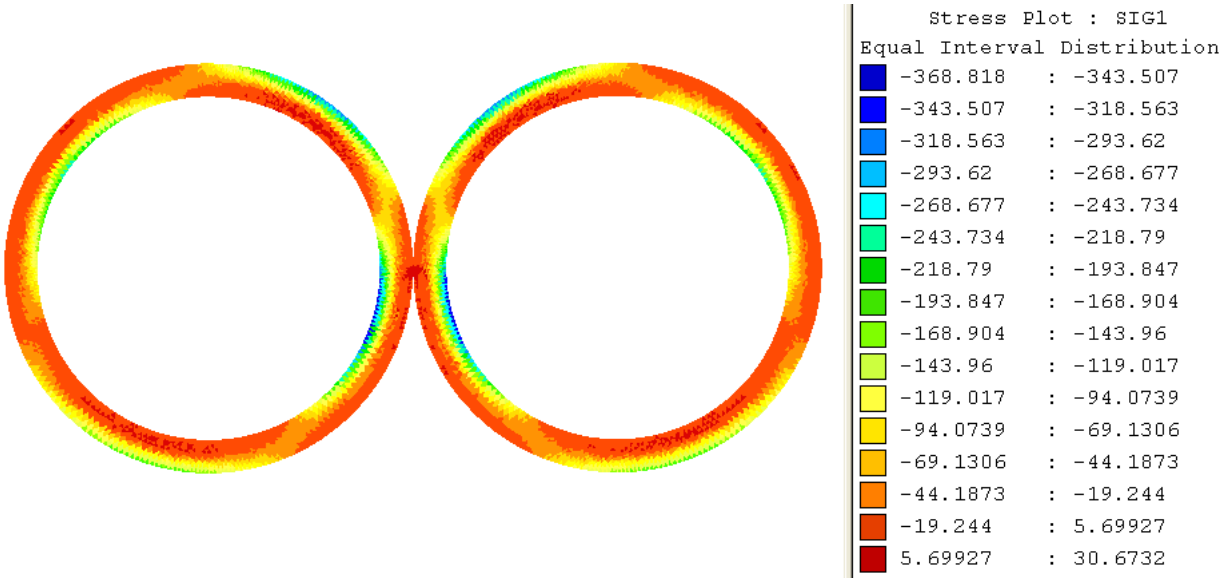

Fig. 6(c) Principal Stress Plot (Largest Compressive Stress) for Load Case 2

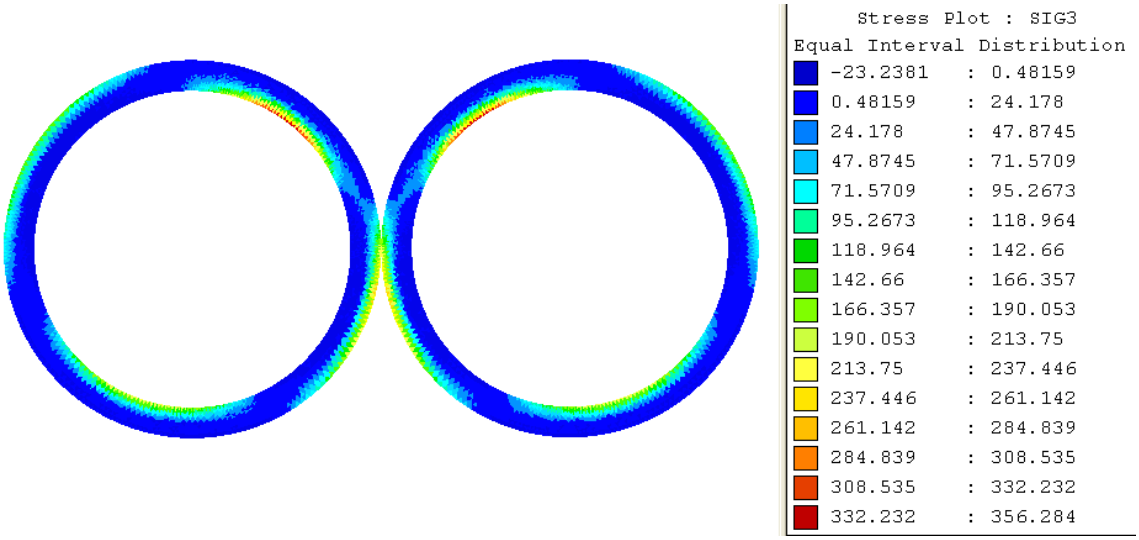

Fig. 6(d) Principal Stress Plot (Largest Tensile Stress) for Load Case 2

2.4 Conclusions

Plane strain analyses were carried out for the pipe subjected to vehicular loading as well as due to the weight of the backfill. The analyses indicate that the largest compressive stress in either pipe is 425 psi and the largest tensile stress in either pipe is 437 psi resulting from Load Case 1. The largest tensile stress occurs at the crown of the pipe directly under the wheel loads. The largest displacements take place in the soil directly under the loading and are 0.4 in for Load Case 1 and 0.5 in for Load Case 2.

3.0 References

[1] HYI, Inc., HYI-3D Finite Element Analysis Program, Phoenix, AZ.
[2] Chandrupatla and Belegundu, Introduction to Finite Elements in Engineering, Prentice Hall, 2002.
[3] Nawy, E.G., Reinforced Concrete – A Fundamental Approach, Prentice Hall, 1996.
[4] Das, Braja, Principles of Geotechnical Engineering, Prentice Hall, 2001.